FATIGUE DAMAGE BEHAVIOUR OF STRUCTURAL COMPONENTS UNDER VARIABLE AMPLITUDE LOADING

H. F. S. G. Pereira[1], A. M. P. Jesus[2], A. S. Ribeiro[3], A. A. Fernandes[4]

[1]Mestre em Engenharia Mecânica, IDMEC - Pólo FEUP, Faculty of Engineering, University of Porto
[2]Prof. Auxiliar, [3]Prof. Associado c/ Agregação, Department of Engineering, University of Trás-os-Montes e Alto Douro
[4]Prof. Catedrático, DEMEGI, Faculty of Engineering, University of Porto


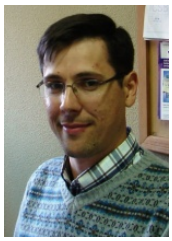

ABSTRACT

The paper summarizes some main results achieved by authors in recent research on fatigue damage behaviour under variable amplitude loading. The fatigue damage behaviour of the P355NL1 steel is investigated as well as of a double sided notched rectangular plate made of P355NL1 steel. Block loading is applied to smooth and notched specimens. Also, constant amplitude loading is applied to derive the basic fatigue strength data for damage calculations according to existing damage rules. Nonlinear fatigue damage evolution with load sequential effects has been found for the P355NL1 steel and for the structural component.

1- INTRODUCTION

Structures are frequently subjected to variable amplitude loading, requiring a fatigue assessment based on damage accumulation rules. The Palmgren-Miner's rule [Miner (1945)] is perhaps the oldest fatigue damage accumulation rule. This damage rule predicts a linear damage evolution, with the number of cycles, and consequently a linear damage accumulation. Due to its simplicity, the linear damage rule still is widely used for design purposes, in spite of its important limitations, such as its insensibility to loading sequence. Most metallic materials exhibit more complex behaviours than modelled by a linear damage rule. Several attempts have been done to propose more reliable fatigue damage rules. Fatemi (1998), Manson (1986) and Schijve (2003) present a comprehensive review about fatigue damage models. However, the new propositions are limited to very specific conditions (e.g. certain loading sequences, materials) hindering the adoption of those rules in current design practices.

It has been verified that metallic materials can exhibit highly nonlinear fatigue damage evolution with load dependency [De Jesus et al. (2005), Pereira et al. (2006a, 2007a, 2007b, 2008)]. This behaviour yields a nonlinear damage accumulation that accounts for loading sequential effects. Thus, depending on load history, the Palmgren-Miner's rule can underestimate or overestimate the fatigue damage.

The main goal of this paper is to report experimental evidence about the fatigue damage accumulation behaviour of the P355NL1 steel and of a structural component made of P355NL1 steel, under variable amplitude loading, in particular under block loading.

2 - FATIGUE DAMAGE MODELLING

2.1 – Linear model

Fatigue life prediction under block loading is generally based on the linear Palmgren-Miner's rule [Miner (1945)]. According to this rule, fatigue damage for constant amplitude block loading can be assessed as follows:

$$D = \sum_{i=1}^{k} \frac{n_i}{N_i} \tag{1}$$

where: D is the accumulated fatigue damage, k is the number of blocks, n_i is the number of constant amplitude cycles applied during the block i characterized by a strain/stress range $\Delta\varepsilon_i/\Delta\sigma_i$, and N_i is the number of cycles to failure that would result for the exclusive application of the loading conditions, $\Delta\varepsilon_i/\Delta\sigma_i$, of block i.

For a sequence of two constant amplitude blocks, the accumulated fatigue damage can be evaluated according the Palmgren-Miner's rule as follows:

$$D = \frac{n_L}{N_L} + \frac{n_H}{N_H} \tag{2}$$

and for multiple alternated constant amplitude block loading as:

$$D = \frac{\sum n_L}{N_L} + \frac{\sum n_H}{N_H} \tag{3}$$

The failure occurs when damage reaches the unity ($D = 1$) in equations (1) to (3).

2.2 – Non-linear model

Some authors [Marco and Starkey (1954)] suggested the replacement of the Palmgren-Miner's rule by the following non-linear relation:

$$D = \left(\frac{n}{N}\right)^{\alpha} \tag{4}$$

where α is a function of the applied load, to be identified on the basis of experimental data. This relation models a non-linear damage evolution with the number of load cycles, as illustrated schematically in figure 1 for a sequence of two constant amplitude blocks. The load dependency of α allows the description of the load sequential effects, also illustrated in figure 1.

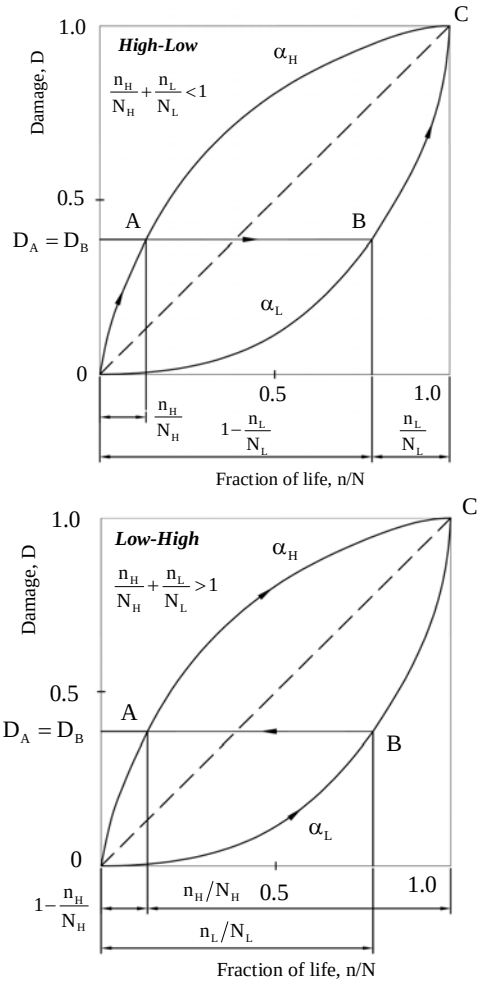

Fig 1 - Illustration of the non-linear damage evolution and load sequential effects for two block loading.

Based on figure 1, it is possible to write the following damage relations, respectively for High-Low and Low-High loading sequences:

<u>High-Low:</u>

$$D_A = D_B \Rightarrow \left(\frac{n_H}{N_H}\right)^{\alpha_H} = \left(1 - \frac{n_L}{N_L}\right)^{\alpha_L} \Leftrightarrow \frac{n_L}{N_L} = 1 - \left(\frac{n_H}{N_H}\right)^{\frac{\alpha_H}{\alpha_L}} \tag{5}$$

Low-High:

$$D_A = D_B \Rightarrow \left(\frac{n_L}{N_L}\right)^{\alpha_L} = \left(1-\frac{n_H}{N_H}\right)^{\alpha_H} \Leftrightarrow \frac{n_H}{N_H} = 1-\left(\frac{n_L}{N_L}\right)^{\frac{\alpha_L}{\alpha_H}} \quad (6)$$

The absolute values of α_L and α_H are not possible to extract using the available data. For this purpose, damage measurements would be required in order to be used with relation (4) [De Jesus et al. (2005)]. Manson and Halford (1986) suggested the following expression for the exponent ratio α_H/α_L:

$$\frac{\alpha_H}{\alpha_L} = \left(\frac{N_H}{N_L}\right)^{0.4} \quad (7)$$

For multiple alternated constant block loading, the following damage relations can be stated based on figure 2:

$$D_1 = a^{\alpha_H} = \left(\frac{n_L^1}{N_L}\right)^{\alpha_L} \Rightarrow \frac{n_L^1}{N_L} = a^{\frac{\alpha_H}{\alpha_L}} \quad (8)$$

$$D_2 = \left(\frac{n_L^1}{N_L}+b\right)^{\alpha_L} = \left(\frac{n_H^2}{N_H}\right)^{\alpha_H} \Rightarrow \Rightarrow \frac{n_H^2}{N_H} = \left(\frac{n_L^1}{N_L}+b\right)^{\frac{\alpha_L}{\alpha_H}} \quad (9)$$

$$D_3 = \left(\frac{n_H^2}{N_H}+a\right)^{\alpha_H} = \left(\frac{n_L^3}{N_L}\right)^{\alpha_L} \Rightarrow \Rightarrow \frac{n_L^3}{N_L} = \left(\frac{n_H^2}{N_H}+a\right)^{\frac{\alpha_H}{\alpha_L}} \quad (10)$$

$$D_4 = \left(\frac{n_L^3}{N_L}+b\right)^{\alpha_L} = \left(\frac{n_H^4}{N_H}\right)^{\alpha_H} \Rightarrow \Rightarrow \frac{n_H^4}{N_H} = \left(\frac{n_L^3}{N_L}+b\right)^{\frac{\alpha_L}{\alpha_H}} \quad (11)$$

(...)

where n_L^1, n_H^2, n_L^3 and n_H^4 are the number of cycles of a "fictitious" constant amplitude loading that induces the same damage as the real loading history, until the application of blocks 1, 2, 3 and 4, respectively. If the failure occurs at the end of the n^{th} block, then, based on equation (4) it is possible to write the following failure relations:

$$D_n = 1 \Rightarrow \begin{cases} \frac{n_H^n}{N_H} = \left(\frac{n_L^{n-1}}{N_L}+b'\right)^{\frac{\alpha_L}{\alpha_H}} = 1 \\ \frac{n_L^n}{N_L} = \left(\frac{n_H^{n-1}}{N_H}+a'\right)^{\frac{\alpha_H}{\alpha_L}} = 1 \end{cases} \quad a' \le a \text{ , } b' \le b \quad (12)$$

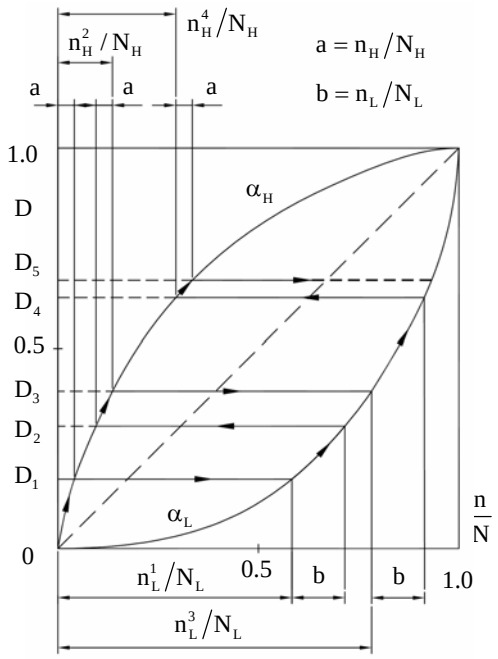

Fig 2 - Illustration of the non-linear damage evolution and load sequential effects for multiple alternated constant amplitude block loading.

This paper proposes the assessment of the linear and non-linear damage rules described above, using experimental data from block loading fatigue tests carried out by the authors.

3 - EXPERIMENTAL DETAILS

The present research is based on an experimental program which included

fatigue tests of both smooth and notched specimens. Both specimens were extracted from plates of P355NL1 steel, supplied with the dimensions of 3140×2000×5.1 mm^3. The P355NL1 steel is intended for pressure vessel applications and is a normalized fine grain low alloy carbon steel. The chemical composition and mechanical properties of the material are given in tables 1 and 2, respectively. The geometries of the specimens are illustrated in figure 3. Specimens were extracted in rolling direction. The geometry of the smooth specimens was defined according to the ASTM E606 standard [ASTM (1986)] . According to Peterson (1959), the notched specimen shows an elastic stress concentration factor equal to 2.17.

All fatigue tests were conducted in an INSTRON 8801 servohydraulic machine rated to 100 kN. The smooth specimens were tested under strain controlled conditions with null strain ratio. In this case, a sinusoidal waveform was applied in all tests with a frequency adjusted to result an average strain rate of $\dot{\varepsilon} = 0.8\%/s$. The strain was measured using an INSTRON 2620-602 clip gauge with a gauge length of ±2.5 mm. The notched specimens were tested under remote stress controlled conditions for R-ratios equal to 0.0, 0.15 and 0.3. Also a sinusoidal waveform was applied.

The failure of the smooth and notched specimens was defined as the complete fracture of the specimens. Both constant amplitude and bock loading were applied to the two types of specimens. Constant amplitude tests were carried out in order to derive the S-N curve for the component. Also two and multiple block loading tests were performed to assess the damage accumulation behaviour of the component. High-Low (H-L), Low-High (L-H), H-L-H-L(…) and L-H-L-H(…) block sequences were investigated. Finally, tests with blocks of variable amplitude loading, following a Gaussian distribution, were carried out.

Table 1 – Chemical composition of the P355NL1 steel (% weight).

C	Si	Mn	P	S	Al	Mo
0.133	0.35	1.38	0.014	0.0016	0.03	0.001
Nb	**Ni**	**Ti**	**V**	**Cu**	**Cr**	
0.025	0.148	0.016	0.002	0.137	0.025	

Table 2 – Mechanical properties of the P355NL1 steel.

Ultimate tensile strength, σ_{UTS} [MPa]	568
Monotonic yield strength, σ_y [MPa]	418
Young's modulus, E [GPa]	205.2
Poisson's ratio, ν	0.275
Cyclic hardening coefficient, K' [MPa]	777
Cyclic hardening exponent, n'	0.1068
Fatigue strength coefficient, σ'_f [MPa]	840.5
Fatigue strength exponent, b	-0.0808
Fatigue ductility coefficient, ε'_f	0.3034
Fatigue ductility exponent, c	-0.6016
Number of transition reversals, N_t	3883
Total transition strain range, $\Delta\varepsilon_t$ [%]	0.84

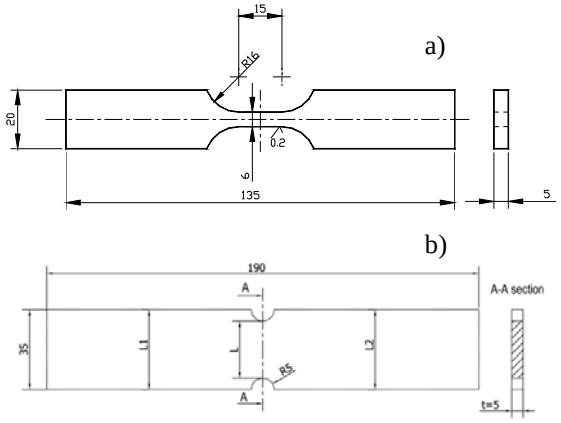

Fig 3 – Geometry of the specimens: a) smooth; b) double notched (dimensions in mm).

4 - EXPERIMENTAL RESULTS AND DISCUSSION

4.1 – Strain controlled tests

The strain controlled fatigue tests were carried out to derive the strain-life behaviour of the P355NL1 steel. These tests were performed for both constant and variable amplitude loading.

4.1.1 – Constant amplitude data

Constant amplitude fatigue tests were carried out in order to derive the low-cycle

fatigue and the cyclic elastoplastic behaviours of the P355NL1 steel. Cyclic tests were carried out for nine predefined strain ranges, namely 0.3%, 0.4%, 0.5%, 0.6%, 0.75%, 1%, 1.5%, 2% and 3%. Fatigue resistance parameters of the P355NL1 steel were determined by fitting the strain-life test data to the Coffin-Manson relation [Coffin (1954), Manson (1954)]:

$$\frac{\Delta\varepsilon}{2} = \frac{\sigma'_f}{E}\left(2N_f\right)^b + \varepsilon'_f\left(2N_f\right)^c \qquad (13)$$

Figure 4 presents the experimental elastic, plastic and total strain amplitudes as a function of the number of reversals to failure. Equation (13) is also plotted in figure 4. As can be observed, equation (13) fits quite well the experimental data. Table 2 lists the fatigue constants used to model the fatigue resistance behaviour of the P355NL1 steel.

The fatigue tests carried out under constant strain amplitude were also useful to characterize the cyclic elastoplastic behaviour of the P355NL1 steel. They exhibited a general stabilized cyclic behaviour for the whole lives and for all tested strain ranges. Only a slight cyclic hardening was detected for the highest strain ranges [Pereira et al. (2007a)].

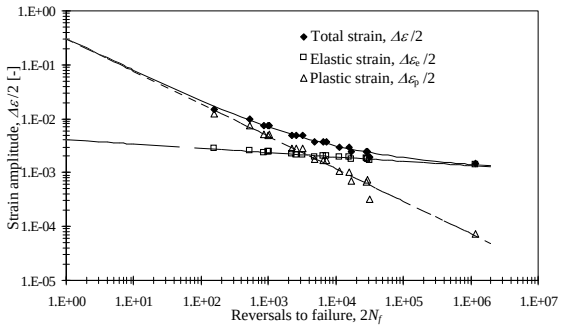

Fig 4 – Constant amplitude strain-life data of the P355NL1 steel (R_ε=0).

4.1.2 – Variable amplitude data

Two types of variable amplitude tests were defined, namely using blocks of constant and variable amplitude strains. Regarding the constant amplitude block loading, two and multiple alternated blocks were applied to the smooth specimens. For the two block loading, the blocks were defined to present distinct strain ranges: a strain range of 1.5 or 1% defines the higher blocks (H); a strain range of 0.75 or 0.5%, defines, respectively, the lower blocks (L). Two loading sequences were investigated, namely the H-L and L-H sequences. The two block loading tests were conducted in such a way that the first block is applied during a predetermined number of cycles, not causing the material failure. Then, the second block is applied until failure. For multiple alternated block loading, the blocks were defined to present the two combinations of strain ranges referred previously: strain ranges of 1.5 or 1% define the higher strain blocks (H); strain ranges of 0.75 or 0.5% defines respectively the lower strain blocks (L). Also, two types of loading sequences were investigated, namely the H-L-H-L(…) and L-H-L-H(…) sequences. Each block has a predefined number of cycles, being alternately applied until the failure is observed (at least two blocks from each strain range were applied).

In addition to the constant amplitude block loading tests, variable amplitude blocks, as illustrated in [Pereira at al. (2007a)], were repeatedly applied, constituting the variable amplitude block loading tests. All variable amplitude tests were carried out under repeated strain controlled conditions (R_ε=0).

Figure 5 illustrates the typical cyclic elastoplastic behaviour of the P355NL1 steel under the H-L block loading. Figure 5a) gives the stress amplitude *versus* cycles. It can be concluded that the material presents an almost stabilized behaviour for both blocks. The transition between the two blocks does not disturb significantly the stabilized behaviour of the material. The stabilized stress amplitudes of figure 5a) are essentially the same of the constant amplitude loading [Pereira et al. (2007a)]. Thus, the application of the block loading does not influence the stabilized stress amplitudes. Figure 5b) presents the evolution of the cyclic mean stress corresponding to the application of the H-L block loading. The application of the first block produces a cyclic mean stress relaxation similar to the one observed for the

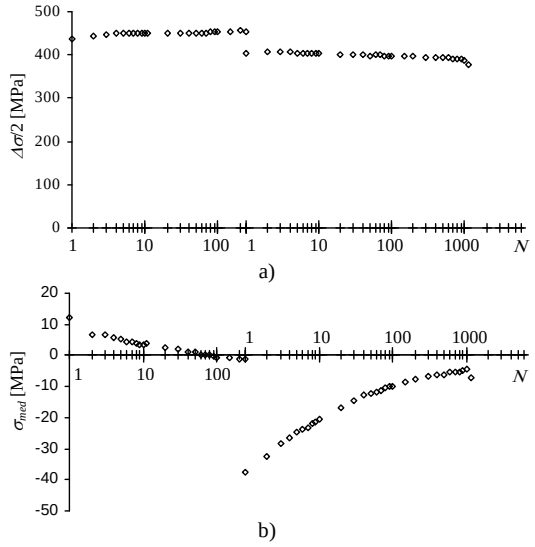

Fig 5 – Elastoplastic cyclic behaviour of the P355NL1 steel under the H-L block loading, with strain ranges of 1.5 and 0.75%: a) stress amplitude *versus* cycles; b) cyclic mean stress *versus* cycles.

constant amplitude tests. However, the transition between the first and the second block results in important compressive cyclic mean stresses. These compressive cyclic mean stresses relax to a relative small compressive mean stress, at failure.

Figure 6 illustrates the experimental data relative to the variable amplitude block loading tests: stress amplitude *versus* cycles and mean stress *versus* cycles. It is worthwhile to note that for the illustrated sequence (H-L), compressive cyclic mean stresses are developed almost after the first cycle, which can be considered beneficial to fatigue. Tests with L-H, L-H-L and random sequences were also performed. They are not reproduced in this paper due to space limitations.

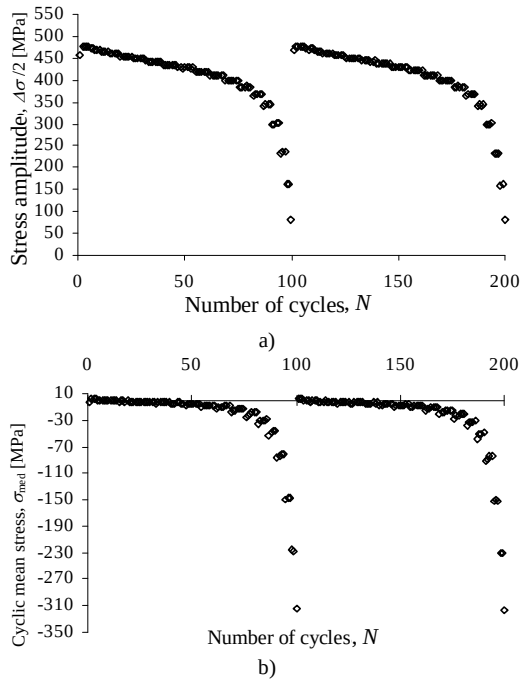

Fig 6 – Elastoplastic cyclic behaviour of the P355NL1 steel under H-L variable amplitude block loading ($\Delta\varepsilon_{max}$=2.1%): a) stress amplitude *versus* cycles; b) cyclic mean stress *versus* cycles.

Figures 7 and 8 illustrate the experimental fatigue data from the constant amplitude blocks. The fractions of lives at higher strain amplitude, n_H/N_H, are plotted against the fractions of lives at lower strain amplitude, n_L/N_L. All figures illustrate the Palmgren-Miner's relation as a straight line resulting from making damage equal to the unity in equations (2) or (3).

The analysis of figure 7a) shows that the investigated material under two block loading data, defined by 0.5 and 1.0% strain ranges, does not follow the linear relation. The figure shows that the material has a non-linear damage accumulation compatible with a non-linear damage evolution, dependent on the loading, as expressed by equation (4). Also, it is possible to observe loading sequential effects. While L-H loading sequences are favourable, H-L loading sequences are detrimental to fatigue life. Equations (5) and (6) were fitted to the experimental data using the least squares fitting technique, resulting the exponent ratio, α_H/α_L=0.18 or α_L/α_H=5.56. It seems that the non-linear damage model gives a very satisfactory description of the experimental data. Manson and Halford proposed an exponent ratio given by equation (7) which results for this case in the following values: α_H/α_L=0.41 and α_L/α_H=2.44. Figure 7a) also includes the curves resulting from equations (5) and (6) with the exponent ratios proposed by Manson and Halford. It can be concluded that this latter representation underestimates the damage accumulation non-linearity.

Figure 7b) illustrates the two block loading fatigue data defined by 0.75 and

1.5% strain ranges. Again, the experimental data deviates from the linear damage model. The best fitting of relations (5) and (6) resulted the following exponent ratios: α_H/α_L=0.56 or α_L/α_H=1.78. The exponent ratio proposed by Manson and Halford results in the following values: α_H/α_L=0.54 and α_L/α_H=2.11. This block loading combination leads to less non-linear damage accumulation than observed for the previous one. The Manson-Halford proposition is very close to the best fit relation.

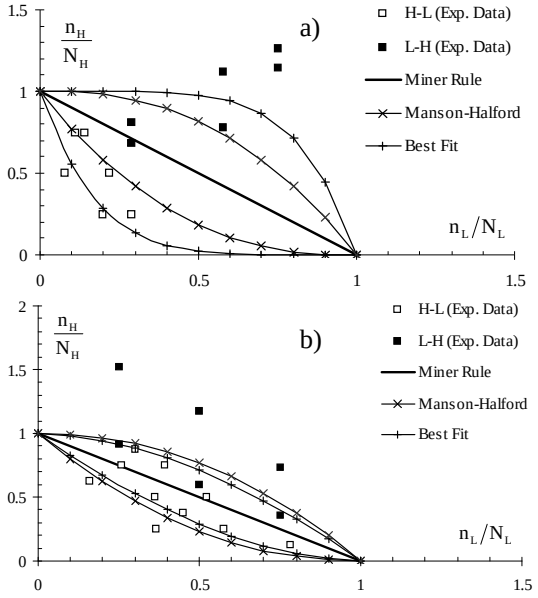

Fig 7 – Fatigue damage data of the P355NL1 steel for two constant amplitude blocks defined by: a) 0.5 and 1.0% strain ranges; b) 0.75 and 1.5% strain ranges.

Figure 8 presents the fatigue data resulted from the multiple alternated block loading, defined respectively by 0.5 and 1.0% and 0.75 and 1.5% strain ranges. For these two situations, the non-linear damage accumulation and the loading sequential effects are not so clear, because for the same loading sequence there are always data points above and below the Palmgren-Miner's line. However, it can be seen that for the 0.5 and 1.0% strain range combinations the L-H-L-H(…) sequences give mean results slightly above the Palmgren-Miner's line; inversely the H-L-H-L(…) sequences give mean results

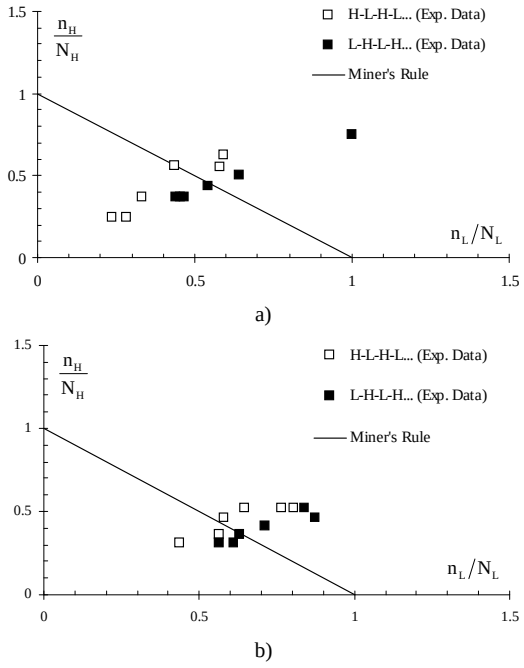

Fig 8 - Fatigue data for multiple alternated constant amplitude blocks loading: a) defined by 0.5 and 1.0% strain ranges; b) defined by 0.75 and 1.5% strain ranges.

slightly below the Palmgren-Miner's line. These results are consistent with the observations done in the two block loading data. For the 0.75 and 1.5% strain ranges, seems that mean data falls above the Palmgren-Miner's relation. This means that the linear relation performs satisfactorily for this situation.

Equations (12) were used to best fit the experimental data, by the least squares technique yielding the damage exponent ratios. Using the data from figure 8a), the following ratios were found: α_H/α_L=2.28 and α_L/α_H=0.44. Data from figure 8b) yields the following ratios: α_H/α_L=1.60 and α_L/α_H=0.62. These exponent ratios are not consistent with the values derived for the two block loading. Thus, despite the non-linear damage model performing satisfactory for two block loading, it does not perform well for multiple alternated block loading.

For the variable amplitude block loading, damage calculations, based on cycle ratio summations, as specified by the linear model, were evaluated and results are presented in table 3. A general trend is

observed – the cycle ratio summations are greater than unity. Thus, the linear model would produce conservative predictions. Also, some results are consistent with observations carried out for the two block loading data. The L-H sequence produces a Miner's damage summation clearly greater than unity; for $\Delta\varepsilon_{max}$=1.05% the H-L sequence yields an average damage slightly lower than unity. For $\Delta\varepsilon_{max}$=1.05% the L-H-L sequence corresponds to an intermediate condition between the H-L and L-H sequences. All sequences with $\Delta\varepsilon_{max}$=2.1% yield an average damage summation greater than unity.

Table 3 – Damage calculations for the variable amplitude block loading tests.

$\Delta\varepsilon_{max}$ (%)	Strain Spectra	Average Damage Summation (Miner's rule)
1.05	(L-H)-(L-H)-(…)	1.337
2.1	(L-H)-(L-H)-(…)	1.534
1.05	(H-L)-(H-L)-(…)	0.953
2.1	(H-L)-(H-L)-(…)	1.607
1.05	(L-H-L)-(L-H-L)-(…)	1.244
2.1	(L-H-L)-(L-H-L)-(…)	1.636
1.05	Random-Random-(...)	0.986
2.1	Random-Random-(...)	1.457

4.2 – Stress controlled tests

Stress controlled tests were carried out to derive the fatigue behaviour of a structural component made of P355NL1 steel. Tests under constant and variable amplitude loading were performed.

4.2.1 – Constant amplitude data

The S-N curves obtained for the structural component under constant stress amplitude and for stress ratios R_σ=0.0, R_σ=0.15 and R_σ=0.3 are plotted in figure 9. The analysis of the figure is conclusive relative to the stress ratio effect. For the same stress amplitude, increasing the stress ratio reduces the fatigue life; conversely, for the same maximum cyclic stress, the fatigue life increases as the stress ratio increases. Table 4 summarizes the C and m constants of the S-N curves defined according to $(\sigma_{\max})^m N = C$. The determination coefficient, R^2, is also included. Finally, the table includes the fatigue endurance limit, σ_{f0}, defined as a cyclic maximum stress.

Table 4 – Parameter of the component *S-N* curves [Pereira et al. (2007b)].

R	m	C	R^2	σ_{f0} [MPa]
0	11.16	2.73E+32	0.9309	200
0.15	10.92	2.39E+32	0.9688	-
0.3	18.35	6.39E+51	0.8295	300

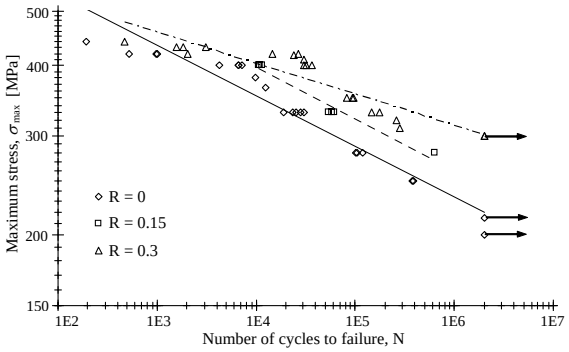

Fig 9 - *S-N* curves for the structural component (maximum stress *versus* cycles to failure).

4.2.2 – Variable amplitude

4.2.2.1 – Constant amplitude blocks

The experimental program included a substantial quantity of variable amplitude tests. These variable amplitude tests were of block and random loading types. Two blocks were applied to the specimens, being each block characterized by constant stress amplitude. Two blocks, multiple blocks and variable amplitude blocks, following a Gaussian distribution, were investigated. The investigated sequences were H-L and L-H, for two block loading, H-L-H-L(…) and L-H-L-H(…), for multiple block loading; for variable amplitude block loading, the investigated sequences were H-L, L-H, L-H-L and random. All tests were carried out under remote stress control. Three stress ratios were investigated, namely R_σ=0.0, R_σ=0.15 and R_σ=0.3.

Figures 10, 11 and 12 illustrate the experimental fatigue data for loading composed by constant amplitude blocks. The fractions of lives at higher stress ranges, n_H/N_H, are plotted against the fraction of lives at lower stress ranges, n_L/N_L. All figures include the linear Palmgren-Miner's curve for comparison

purposes. It is clear, by the analysis of figures, that the structural component does not follow the linear damage model. The fatigue damage evolves nonlinearly with the number of cycles. For R_σ=0 (see figures 10a) and 10b)) the fatigue damage is also a function of the loading as defined by relations (4)-(6) and the loading sequential effects are clearly visible. On effect, for the H-L loading sequences, the summation of the fractions of lives is lower than unity; for the L-H sequences the summation of the fractions of lives is higher than unity. The best fit of experimental data for R_σ=0 resulted the damage exponent ratios of α_L/α_H=2.22 and α_H/α_L=0.45, for the combination of 280 and 400 MPa stress ranges, and α_L/α_H=2.07 and α_L/α_H=0.48, for the combination of 280 and 330 MPa stress ranges. These damage exponent ratios are consistent with the values obtained for the P355NL1 steel, with respect to the loading sequential effects [Pereira et al. (2006a, 2007a, 2007b)].

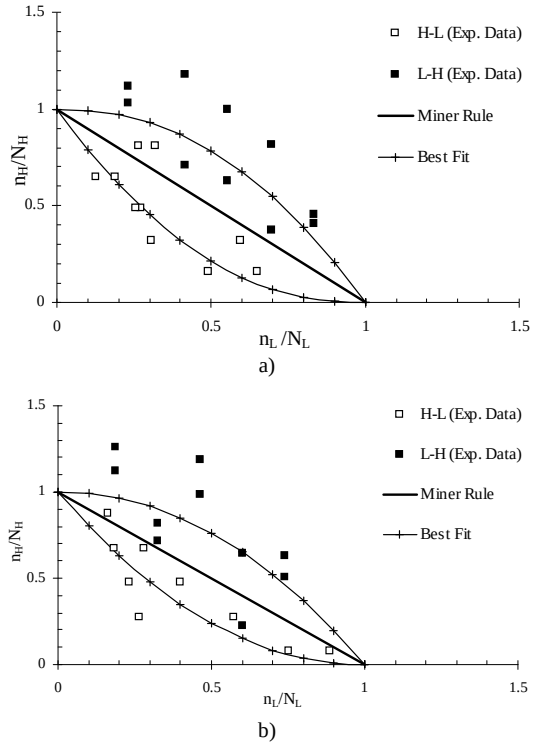

Fig 10 - Fatigue data for two block loading: a) defined by 280 and 400 MPa stress ranges (R_σ=0); b) defined by 280 and 330 MPa stress ranges (R_σ=0).

Surprisingly, there is an important stress ratio influence on the loading sequential effects. For R_σ=0.15 and R_σ=0.3 there is no appreciable loading sequential effects on damage accumulation, as illustrated by figures 11a) and 11b). The damage relation (4) fails to predict this behaviour. It seems that the damage exponent α is no longer a load function. For these two stress ratios the Palmgren-Miner's linear relation seems to be conservative, since all experimental failure data points lay above it.

For multiple block loading, figure 12a) and 12b) show that the component is not sensible to the loading sequence. For multiple block loading with R_σ=0, the Palmgren-Miner's linear relation is essentially non conservative, but for R_σ=0.3 the Palmgren-Miner's linear relation is significantly conservative.

4.2.2.2 – Variable amplitude blocks

The experimental program composed of blocks of variable amplitude loading consisted on the application of several short constant amplitude blocks or random loading following a Gaussian distribution. Tests with stress ratios of R_σ=0, R_σ=0.3 and random, were carried out. The investigated sequences were the H-L, L-H, L-H-L and random. For tests with random *R*-ratios, the cycles counting was performed using the FATVEN [Pereira et al. (2006b)] software which is based on the reservoir cycle counting method [CEN (2002)].

For the variable amplitude block loading, damage calculations, based on cycle ratio summations, as specified by the linear model, were evaluated and results are presented in table 5. A general trend is observed – the cycle ratio summations are greater than unity. For random sequences, the cycle ratio summations are near to unity. Thus, the linear model would produce conservative predictions. Also, some results are consistent with observations carried out for block loading data.

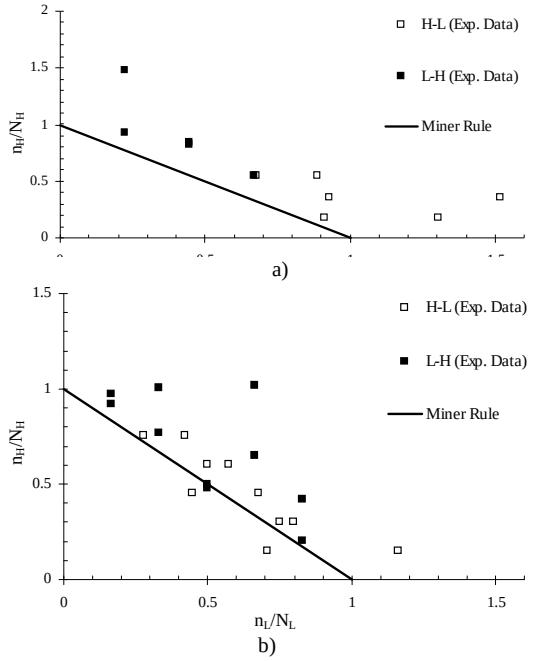

Fig 11 - Fatigue data for two block loading: a) defined by 280.5 and 340 MPa stress ranges (R_σ=0.15); defined by 245 and 280 MPa stress ranges (R_σ=0.3).

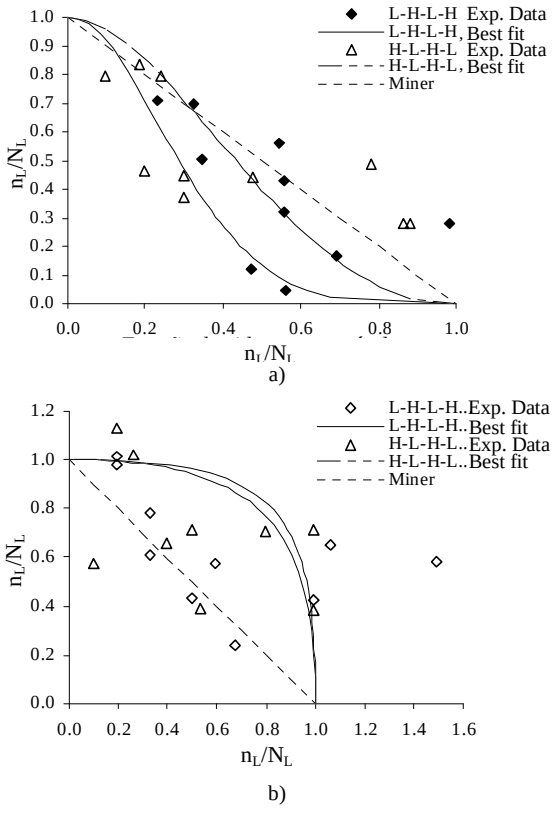

Fig 12 - Fatigue data for multiple block loading: a) defined by 330 and 280 MPa stress ranges (R_σ=0); defined by 245 and 280 MPa stress ranges (R_σ=0.3).

Table 5 - Damage calculations for the variable amplitude block loading tests with R_σ= 0.

$\Delta\sigma_{max}$ (MPa)	Sequence	Stress ratio R_σ	Average damage Summation (Miner's Rule)
420	H-L	0	1.0915
420	L-H	0	0.8413
420	L-H-L	0	1.2380
420	Random	0	0.9157
420	H-L	0.3	1.485
420	L-H	0.3	1.476
420	L-H-L	0.3	2.329
420	Random	0.3	0.741
420	Random	Random	1.139
420	Random	Random	0.852

5 – CONCLUDING REMARKS

This paper presented an assessment of fatigue and fatigue damage accumulation data of the P355NL1 steel as well as of a structural component made of P355NL1 steel. Constant amplitude, constant amplitude block loading and variable amplitude block loading data was assessed. The application of two constant amplitude blocks demonstrated that the material exhibits non-linear damage accumulation behaviour with load sequential effects, which is consistent with a non-linear damage evolution with the number of cycles. For this particular loading, the Palmgren-Miner's rule produces clearly inconsistent results. A non-linear damage rule as the one proposed by Marco and Starkey seems to be a proper choice. However, this rule fails to model the damage accumulation behaviour for the multiple alternated constant amplitude block loading. This suggests that for loading histories approaching the random type are fairly modelled by the liner damage rule.

In a general way, loading histories beginning with a H block loading are more damaging than sequences starting by L blocks.

The variable amplitude block loading was characterized by cycle ratio summations greater than unity, which turns the Palmgren-Miner's law conservative.

Regarding the fatigue damage accumulation for the structural component,

it was observed for R_σ=0 a damage behaviour compatible with a non-linear damage evolution, function of the stress cycles and dependent on loading. This behaviour is responsible for a non-linear damage summation with loading sequential effects.

For R_σ=0.15 and R_σ=0.3 the structural component did not exhibit loading sequential effects on fatigue damage summation. For these two latter stress ratios the Palmgren-Miner's relation yields safe predictions.

For variable amplitude loading the structural component present in general cycle ratios summation greater than unity.

Significant scatter is observed on experimental data. However, it can be considered usual in variable amplitude loading fatigue tests of components.

REFERENCES

Miner, M.A., "Cumulative Damage in Fatigue", Journal of Applied Mechanics, Vo. 67, pag. A159-A164, 1945.

Fatemi A., Yang L., "Cumulative fatigue damage and life prediction theories: a survey of the state of the art for homogeneous materials", Int. J. of Fatigue, Vo. 20, nº 1, pag. 9-34, 1998.

Schijve, J., "Fatigue of structures and materials in the 20th century and the state of the art", Materials Science, Vo. 39, nº3, pag. 307-333, 2003.

De Jesus, A.M.P., Ribeiro, A.S, Fernandes, A.A., "Finite Element Modeling of Fatigue Damage Using a Continuum Damage Mechanics Approach", J. of Pressure Vessel Technology, Vo. 127, nº2, pag. 157-164, 2005.

Pereira, H.F.G.S., De Jesus, A.M.P., Fernandes, A.A. and Ribeiro, A.S, "Fatigue Damage under Block Loading", 5th International Conference on Mechanics and Materials in Design, Porto, Portugal, 24-26 July, 2006a.

Pereira, H.F.G.S., De Jesus, A.M.P., Fernandes, A.A. and Ribeiro, A.S, "Cyclic and Fatigue Behaviour of the P355NL1 Steel Under Block Loading", 2007 ASME Pressure Vessels and Piping Division Conference, S. Antonio, Texas, USA, 2007a.

Pereira, H.F.G.S., De Jesus, A.M.P., Fernandes, A.A. and Ribeiro, A.S, 2007, "Fatigue damage behaviour of a structural component made of P355NL1 steel under block loading", 2007 ASME Pressure Vessels and Piping Division Conference, S. Antonio, Texas, USA, 2007b.

Pereira, H.F.G.S., De Jesus, A.M.P., Fernandes, A.A. and Ribeiro, A.S, "Fatigue Analysis of fatigue damage under block loading in a low carbon steel", STRAIN, 2008, in press.

Marco, S.M., Starkey, W.L., "A Concept of Fatigue Damage" Translations of the ASME, 76(4), pp. 627-632, 1954.

Manson, S.S., Halford, G.R., "Re-examination of cumulative fatigue damage analysis - an engineering perspective", Engineering Fracture Mechanics, Vo. 25 pag. 538-571, 1986.

ASTM: American Society for Testing and Materials. ASTM E606, "Standard Practice for Strain-Controlled Fatigue Testing", Annual Book of ASTM Standards, Vol. 03.01 ASTM, West Conshohocken, PA, pp. 557-571, 1986.

Peterson, R.E., "Notch sensitivity", Metal Fatigue, Sines, G. and Waisman, J.L., edition, McGraw-Hill Book Company, Inc., New York, pp. 293-306, 1959.

Coffin, L.F., "A study of the effects of cyclic thermal stresses on a ductile metal", Translations of the ASME, 76, pp.931-950, 1954.

Manson, S.S., "Behaviour of materials under conditions of thermal stress", NACA TN-2933, National Advisory Committee for Aeronautics, 1954.

Pereira, H.F.S.G., de Jesus, A.M.P., Fernandes, A.A., Ribeiro, A. S., "Sotware development for fatigue assessment of unfired pressure vessels according to the en13445 standard", Proceedings of 10th Portuguese Conference on Fracture, ISBN: 972-99596-1-7, Guimarães, 22-24 Fevereiro, 2006b.

European Committee for Standardization - CEN, "EN 13445: Unfired Pressure Vessels", European Standard, 2002.